Available online at www.sciencedirect.com
SCIENCE DIRECT
Gene 359 (2005) 63 – 72
GENE
SECTION
FUNCTIONAL GENOMICS
www.elsevier.com/locate/gene

Identification, expression analysis, genomic organization and cellular location of a novel protein with a RhoGEF domain

Sze-Wah Tse [a], Jennifer A. Broderick [a], Mei-Ling Wei [a], Min-Hua Luo [a,b], Deborah Smith [a], Peter McCaffery [a,c], Stefan Stamm [d], Athena Andreadis [a,c,*]

[a] Department of Biomedical Sciences, E.K. Shriver Center for Mental Retardation, Waltham, MA 02452, United States
[b] Department of Microbiology, Xiangya Medical School, Central South University, Changsha 410078, Hunan, P.R. China
[c] Department of Cell Biology, University of Massachusetts Medical School, Worcester, MA 02116, United States
[d] University of Erlangen-Nurenberg, Institute of Biochemistry, 91054 Erlangen, Germany

Received 21 March 2005; received in revised form 17 May 2005; accepted 3 June 2005
Received by A.J. van Wijnen

Abstract

In this study we describe the identification and characterization of a novel cytosolic protein of the guanine exchange factor (GEF) family. The human cDNA corresponds to predicted human protein FLJ00128/FLJ10357 located on chromosome 14q11.2. The deduced protein sequence contains in its C-terminus a RhoGEF domain followed by a pleckstrin domain. Its N-terminus, central region and RhoGEF/pleckstrin domain are homologous to the recently identified zebrafish Quattro protein, which is involved in morphogenetic movements mediated by the actin cytoskeleton. Based on the homology of our protein's RhoGEF domain to the RhoGEF domains of Trio, Duo and Duet and its homology with Quattro, we named it Solo. The Solo mRNA is ubiquitously expressed but enriched in brain, its expression peaks perinatally and it undergoes extensive alternative splicing. In both myoblasts and neuroblastoma cells, the Solo protein is concentrated around the nucleus.

Keywords: Yeast two-hybrid screen; FLJ protein; Alternative splicing; Perinuclear localization

1. Introduction

Guanine exchange factors (GEF) stimulate Rho and Rac signal transduction molecules by switching them from the inactive (GDP-bound) to the active (GTP-bound) form. These molecules are often involved in organizing the cytoskeleton and act as axon guidance molecules (Schmidt and Hall, 2002). In a yeast two-hybrid screen aimed to identify proteins interacting with the hinge domain of tau, we isolated a cDNA corresponding to predicted human protein FLJ00128/FLJ10357. Here we report the genomic organization, expression analysis and cellular localization of this novel gene and its product, which we named Solo to reflect its homology to Duo, Duet, Trio and Quattro (members of the RhoGEF superfamily; Erickson and Cerione, 2004). The C-terminus of the deduced Solo protein sequence contains a RhoGEF domain followed by a pleckstrin domain, and three of its regions are homologous to equivalent regions of the zebrafish Quattro protein, which is involved in morphogenetic movements mediated by the actin cytoskeleton (Daggett et al., 2004). The Solo transcript varies in different tissues and developmental stages and also undergoes extensive alternative splicing, which influences the length of its reading frame.

2. Materials and methods

2.1. Yeast two-hybrid assay

We used the Clontech GAL4 yeast two-hybrid system to identify proteins interacting with the hinge region of tau.

Abbreviations: EST, expressed sequence tag; GEF, guanine exchange factor; PH, pleckstrin domain.

* Corresponding author. Shriver Center, 200 Trapelo Road, Waltham, MA 02452, United States. Tel.: +1 781 642 0279; fax: +1 781 642 0017.
E-mail address: Athena.Andreadis@umassmed.edu (A. Andreadis).

0378-1119/$ - see front matter © 2005 Elsevier B.V. All rights reserved.
doi:10.1016/j.gene.2005.06.025

The bait contained human tau exons 5 and 6 (56 and 198 nt, respectively) and the first 80 nucleotides of tau exon 7. To prepare it, we inserted a 230 bp EcoRI/NotI tau cDNA fragment into vector pGBT9 (Clontech). Afterwards, we filled in the EcoRI site to create an AseI site, so that the fusion protein would have the correct reading frame in its tau portion.

The 5/6/7 bait and a rat brain (day P6) library in vector pGAD424 (Clontech) were serially transformed into yeast reporter strain HF7c, which was plated on SD plates lacking tryptophan, leucine and histidine (the reporter gene). The clones which grew in the absence of histidine were further tested for lacZ activity (development of blue color on plates containing X-gal). The library plasmids contained in the positive yeast colonies were isolated by passage through the leuB$^-$ *E. coli* strain HB101 (selected for leucine prototrophy on M9 minimal medium). Plasmid DNA was produced by Qiagen Tip-50 s and sequenced in an ABI fluorescent sequencer using either primers specific to GAD424 or primers from the Solo sequence.

2.2. cDNA cloning, sequencing and sequence analysis

We isolated two unique clones from the two-hybrid screen. One codes for TIF1, which is involved in transcriptional regulation (Le Douarin et al., 1997). The other, which we originally named mp31, codes for a novel protein with RhoGEF and pleckstrin domains at its C-terminal region. For reasons described in Results, we eventually decided to call this molecule Solo.

Since yeast hybrid systems contain fusion proteins which de facto lack the 5′end, we used the 5′most 300 nucleotides of mp31 to screen a rat testis library (Clontech). This yielded three clones, 16-1, 6-7 and 1-17; the latter contained a significant length of additional 5′sequence past mp31. We then used the 5′end of 1-17 to search two cDNA libraries, rat testis (Clontech) and rat adult brain (Stratagene) for clones extending 5′wards. The screenings yielded a cDNA, Solo 1-17, which minimally extended Solo. At that point, no rat libraries yielded any more clones extending upstream; however, a human EST from the Japanese HUGO base clearly showed a longer ORF. So we used PCR techniques to probe a mouse cerebellum cDNA library (Incyte) which gave us a short additional 5′end sequence.

At that point, the genomic version of Solo became available for both human and mouse. We used the combined cDNA sequence of all the clones to search for the corresponding mouse and human genomic sequence in the GenBank database. Alignment analysis, based on loss of contiguity between the cDNA and genomic segments and on the presence of typical 5′ and 3′ splice site motifs, was carried out to determine the exon/intron boundaries (shown in Table 1). Comparisons of the two genomic

Table 1
Solo exon/intron organization—mouse (human)

Exon	C	3′ss cagG	Exon length (bp)	5′ss CAGgtragt	C	Intron length (kbp)	Comments/features
1	?	?	>110	ATGgtgagt	7/9	2.6	ATG
2	4/4	cagG	198	TGTgtgagt	6/9	1.2 (0.7)	
3*	4/4	cagG	1237 (1249)*	CAGgtgaga	8/9	0.11*	
4	4/4	cagG	168	CTGgtcagt (CGGgtcagt)	7/9	0.75 (0.15*)	
5	4/4	cagG	127 (121)	TAGgtaagc (CAGgtaacc)	7/9	0.6	
6*	4/4	cagG	97	CAGgtaatc (CAGgtaacc)	7/9	0.11*	
7*	4/4 (3/4)	cagG(tagG)	81	CAGgttggt (CAGgttgag)	7/9 (5/9*)	0.12*	
8	4/4	cagG	117	CAGgtaaac (CAGgtaagc)	7/9 (8/9)	2.0 (1.3)	
9*	4/4	cagG	96	GAGgtatgg (GAGgtatga)	6/9	0.09* (0.11*)	
10	4/4	cagG	116	CAAgtaaga (CAAgtacga)	7/9 (6/9)	0.5 (0.4)	
11	4/4 (3/4)	cagG (aagG)	127	CAGgtaaag (CAGgtgagc)	7/9 (8/9)	1.1 (1.65)	
12*	4/4	cagG	123	CAGgtaagg (CAGgtgaga)	8/9	0.08* (0.9)	
13	4/4	cagG	144	CAGgtgagg (CAGgtgcat)	8/9 (6/9)	0.5	
14*	3/4	tagG	611	CAGgtgaga	8/9	0.12*	
15	3/4	cagC (cagT)	235	CATgtgagc (CACgtgagt)	7/9 (8/9)	0.3 (0.35)	
16	4/4	cagG	87	AAGgtaaac (AAGgtaact)	6/9 (7.9)	>2.3 (0.9)	
17	3/4	tagG	216	GAGgtaagg (GAGgtgagg)	7/9	0.8 (0.7)	
18	3/4	cagA	171	AAGgtgtgc (AAGgtacga)	6/9	1.3 (0.8)	
19	3/4	cagA	178	AGGgtaacg (AGGgtactg)	5/9	1.2 (1.15)	
20	2/4* (3/4)	tagA (cagA)	105	GAGgtgagg	7/9	0.2	
21	3/4	cagC	144	TGGgtgagg	6/9	0.2	
22a*	2/4*	tagC	132 (135)	CTTgttagg (TTGgtaggg)	5/9*	0.15*	TAA (CAA)
22b	3/4	cagC	131	CAGgtgagt (CAGgtaagt)	9/9	0.25 (0.7)	
Mini*	3/4	tagG	21*	AAGgtcaga	5/9*		Functional 3′ss only in mouse
23	3/4	cagA	47	TAGgtgagt (TGGgtgagt)	8/9 (7/9)	0.3	TGA
24	4/4	cagG	>300	?			

The items in parentheses show the properties of the human exon, if different from the mouse.
C=agreement of splice sites with the consensus sequence.
*=unusual features (very short or long exon, very short intron, very low splice site agreement with consensus).

sequences against all available cDNAs and ESTs convinced us that we had identified the full open reading frame of Solo, although the question of additional untranslated exons remains open.

2.3. Northern and RT-PCR analysis

We analyzed Solo mRNA expression by using a multiple-tissue Northern blot of adult rat (Clontech) and mouse developmental blots. For the latter, we prepared mouse RNA from mouse embryos at defined developmental points and from selected adult mouse tissues by the TRIzol method (Invitrogen) and performed Northern blot analysis. We ran two sets of the mouse developmental Northern panels and normalized the Solo mRNA levels against the 28 S rRNA. As probes, we used: for the rat, the mp31 rat cDNA labeled by the random priming method and [^{32}P]-dCTP (Mega-Prime kit, Amersham); for the mouse, the 810 bp insert of mouse Solo EST AI391306 labeled with Digoxigenin following the manufacturer's instructions (Roche).

To determine if Solo is alternatively spliced beyond the variations that we gleaned by scanning the EST database, we reverse-transcribed 1 μg of human poly A$^+$ RNA from various tissues (Clontech) using RNAase H-superscript (Invitrogen), in 20 μl for 1 h at 42 °C. 1 μl of this reaction mix was then added to ready-to-go PCR beads (Pharmacia) in a total volume of 25 μl with desired primer pairs (shown in Table 2). Conditions used for the PCR were: denaturation at 94 °C for 1 min, annealing at 60–68 °C for 1 min (depending on the primers), elongation at 72 °C for 1 min, 25 cycles. We cloned selected RT-PCR products into vector PCR4-Topo (Invitrogen), prepared plasmid DNA using Qiagen tip-25 columns and had them sequenced in an ABI fluorescent sequencer.

2.4. Antibody production and Western blot analysis

We prepared and affinity-purified polyclonal antibodies against two peptides of the Solo protein (shown in red in Fig. 1A). One is an IgG raised in rabbit against peptide ERRIQQQLGEEASPRSHRR in Solo exon 14 (Zymed). The other is an IgY raised in chicken against peptide LHEQVVVQLAALPWQL in Solo exon 3 (J-QUE Biologics, Worcester, MA).

To detect the distribution of Solo protein in tissues, we obtained various protein medleys from human tissues from Clontech (fetal brain, whole adult brain, cerebellum, cerebral cortex, hippocampus, thalamus, spinal cord, skeletal muscle and liver). 18 μl of each protein sample (protein concentration 10 mg/ml) with 5 mM DTT added were boiled, run on 12% SDS-PAGE gel, and transferred to 0.45 μm nitrocellulose membrane (Osmonics Inc.) using a Bio-Rad Trans-Blot. The blot was then blocked in TBST buffer (20 mM Tris–pH 7.5, 150 mM NaCl, and 0.05% Tween 20) containing 5% non-fat dry milk at room temperature for 1 h. It was then incubated with chicken anti-Solo antibody (1:5000) overnight at 4 °C, washed 6×, 15 min each, with TBST containing 5% non-fat dry milk; incubated with HRP-conjugated rabbit-anti-chicken secondary antibody (1:5000, Zymed) for 1 h at room temperature, washed 3×, 10 min each, with TBST; and detected with enhanced chemiluminescence ECL reagent (Perkin Elmer).

Table 2
Primers used in PCR

Name	Strand	Location	Length	Sequence
a. Cloning (Incyte library)				
Forward	S	In Solo1-17 clone	27	TCCATGGAGCCTGAACCAGTGGAGGAC
Reverse	A	In Solo1-17 clone	27	TACCTGCAGGTAGAAGTCTCCAGGGCG
b. RT-PCR of human Solo RNA				
Solo-E2S	S	Human Solo exon 2	30	GAGCCTGAGCCAGTGGAGGACTGTGTGCAG
Solo-E4S	S	Human Solo exon 4	30	CTGTCTGACACTCCAACACCTCCGCTGGAG
Solo-E4N	A	Human Solo exon 4	30	GTCAGGATGAGGAATCCAGATGCCATCAAG
Solo-E8S	S	Human Solo exon 8	30	GGTGCTGAGGTGCTGTCAGAGAATGATCTG
Solo-E8N	A	Human Solo exon 8	30	CTGGTGTATCTCTACCCAGTGACTGGGAGA
Solo-E13S	S	Human Solo exon 13	30	GCTCTGGAGGAGAATGCCACCTCCCAGAAG
Solo-E13N	A	Human Solo exon 13	30	CTGCTGGAAGAAGCGCTGTAGCCGCAGGGC
Solo-E15S	S	Human Solo exon 15	30	CAGCGGCTGGTGTCTGAGCTGATTGCCTGT
Solo-E15N	A	Human Solo exon 15	30	CTGAAGCTCCCGCAGAAAGTGTGTCCGGTG
Solo-E18S	S	Human Solo exon 18	30	ATAGATCTGAAGGAGCAGGGACAGCTCTTG
Solo-E18N	A	Human Solo exon 18	30	CTTGCTGAACAGGAGGAGATGCTCGAAGAG
Solo-E20S	S	Human Solo exon 20	30	AGCTCCGAGTGCAGCAGATGGTGTCCATGG
Solo-E21S	S	Human Solo exon 21	30	GTGGCCGTGTCATCCTTTGAGCATGCCGGC
Solo-E21N	A	Human Solo exon 21	30	ATTTGCTTGACGTCCAGATCCCAGGCCTCC
Solo-E23N	A	Human Solo exon 23	24	GTCACTCAGGGCTCGAGCATGACT
Solo-E24N	A	Human Solo exon 24	30	GAGAAGCTGCACGCAAGTTCTGGATCTTCT

S=sense, A=antisense.

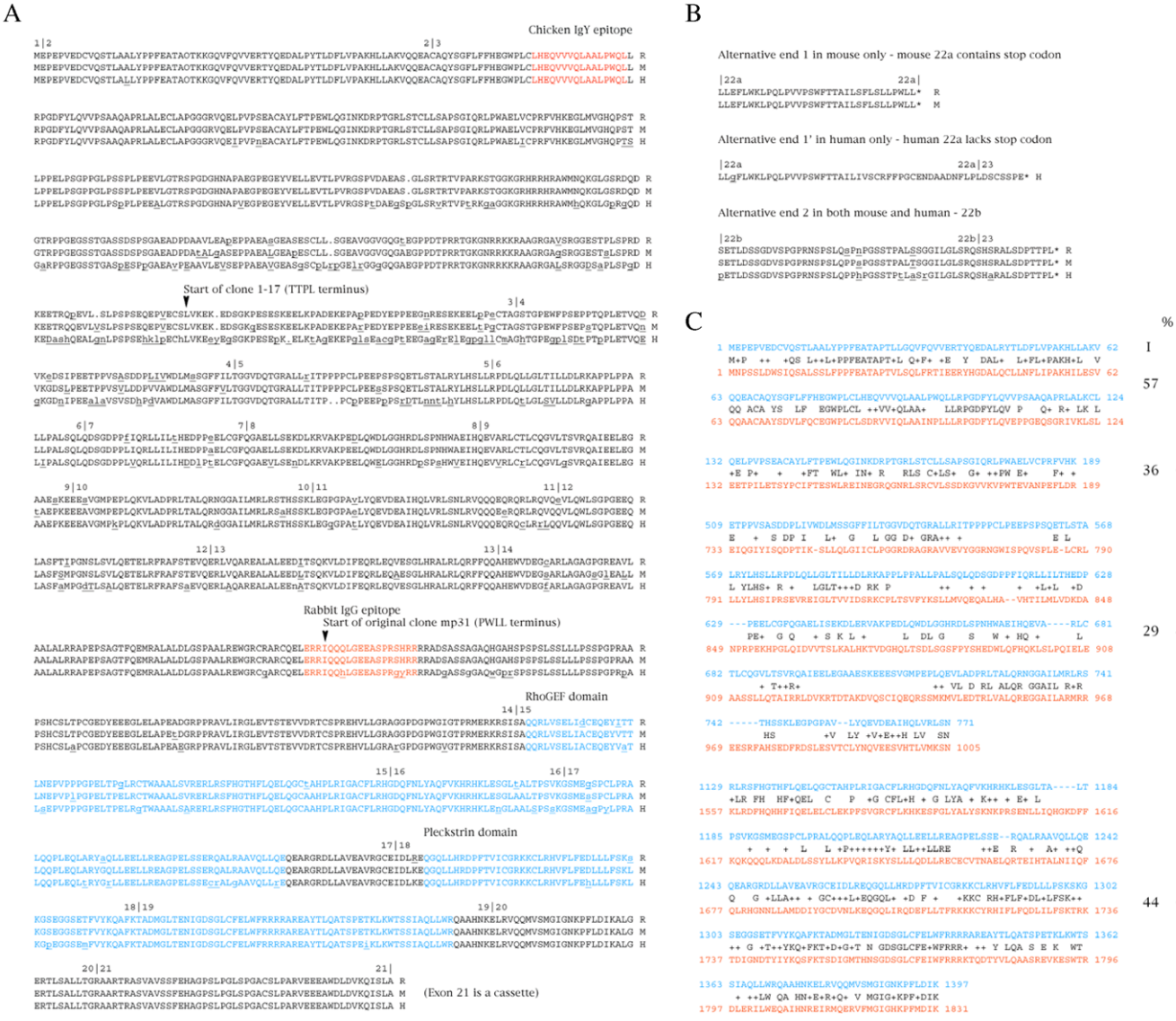

Fig. 1. (A) Comparison between rat (R), mouse (M) and human (H) Solo. Differences in amino acids are underlined and in uppercase if conservative, lowercase if not. The RhoGEF and pleckstrin domains are in blue and the epitopes used to generate antibodies are in red. The starts of the two major rat cDNA clones and the exon boundaries are indicated. (B) The different C-termini generated by alternative splicing of exons 22a and 22b. (C) The homologies between rat Solo and zebrafish Quattro. The last homology contains the RhoGEF and pleckstrin domains. The numbers on the right show percent identity (I) and conservation (C) between Solo and Quattro in the four regions.

2.5. Co-immunoprecipitation of Solo and tau

To test independently if the mp31 peptide interacts with tau, we cloned an insert almost identical to the mp31 insert sequentially first into EGFP-C1 (Clontech), then into pCMV-Tag2C (Stratagene). The insert is longer than mp31 by 18 nucleotides and has an engineered EcoRI site at its 5′ end. After confirming protein expression by Western blotting, the FLAG/Solo construct was co-transfected with two FLAG/fetal tau (FFT) constructs lacking exons 2, 3 and 10: FFT/6^{+} (with exon 6) and FFT/6^{-} (without exon 6) (Luo et al., 2004).

COS cells were maintained in Dulbecco's modified Eagle Medium (DMEM, Invitrogen) supplemented with 10% fetal calf serum. Plates that had reached ~70% confluence were co-transfected with 5 μg of FLAG/Solo and of FFT/6^{+} or FFT/6^{-} DNA using the lipofection method (LT1, Mirus). The medium was changed after 18 h and cells were harvested 36 h after transfection. Cells were washed with phosphate-buffered saline (PBS, Invitrogen), lysed in lysis buffer (150 mM NaCl, 0.1% NP-40, 50 mM Tris) containing 1× protease inhibitor cocktail (Roche), and centrifuged at 4 °C for 10 min at 12,000 rpm.

The supernatant was pre-cleared with 25 μl Agarose G beads (Roche) at 4 °C for 3 h to reduce background. The pre-cleared extract was incubated with 1.5 μg Tau-12 antibody and 25 μl agarose G beads at 4 °C overnight. The beads were washed extensively twice with lysis buffer containing 150 mM NaCl, twice with buffer containing 300 mM NaCl and once with lysis buffer

containing 150 mM NaCl. The bound protein was boiled, loaded on a 10% SDS-PAGE gel and subjected to Western blot analysis (as described before). The primary antibody used was rabbit-anti-FLAG (1:5000, Sigma), the secondary goat-anti-rabbit IgG (1:5000, Zymed).

2.6. Immunocytochemistry

SY5Y (human neuroblastoma cells) and C2C12 (mouse myoblasts) were grown on slides, which were rinsed three times with PBS and then fixed in PEM (80 mM PIPES, 5 mM EGTA, 1 mM $MgCl_2$, pH 6.8) containing 0.3% glutaraldehyde at 37 °C for 15 min. After fixation, cells were rinsed once with PBS, permeabilized with PBS containing 0.5% Triton X-100 for 15 min at room temperature and blocked in PBS containing 10% normal goat serum at room temperature for 1 h.

Cells were stained either for Solo alone or for Solo plus (individually) tau, tubulin or actin. After blocking, cells were incubated with primary antibody for 1 h at room temperature, washed with PBS 5× for 5 min, then incubated with rabbit anti-chicken IgG for 1 h at room temperature. All primary antibodies were diluted in blocking solution. For C2C12 cells, dilutions were 1:100 for polyclonal chicken-anti-Solo; 1:200 for mouse monoclonal tau-5 (Chemicon); 10 μg/ml for α-tubulin (Zymed) and 1 unit/ml for phallotoxin (Molecular Probes) for labeling of f-actin. For SY5Y cells, dilutions were 1:300 for chicken-anti-Solo, 1:600 for tau-5, 3.3 μg/ml for α-tubulin, and 0.5 unit/ml for phallotoxin.

Secondary antibodies were all from Molecular Probes and they were diluted 1:500 in blocking solution. After washing with PBS 5× for 5 min, cells were incubated in Alexa fluor 488 goat-anti-rabbit and Alexa fluor 555 goat-anti-mouse IgGs for 1 h at room temperature, followed by five PBS washes, 5 min each. To double label endogenous Solo and f-actin, Alexa fluor 546 conjugated phallotoxin was used instead of Alexa fluor 555 goat-anti-mouse in the secondary antibody incubation step. The slides were then drained, dried, mounted with gelmount, and observed under a fluorescent microscope.

3. Results

3.1. Sequence analysis, chromosomal location and genomic organization of Solo

The mp31 cDNA encodes a novel protein with RhoGEF and pleckstrin (PH) domains at its C-terminal region. These domains are found in proteins which stimulate Rho and Rac signal transduction molecules by switching them from the inactive (GDP-bound) to the active (GTP-bound) form. These molecules often help to organize the cytoskeleton and act as axon guidance molecules (Schmidt and Hall, 2002). Among them are Duo (Huntingtin-associated protein interactor 1), Duet and Trio (kalirin, unc73). In keeping with this naming tradition, we decided to call our novel gene product Solo—an inadvertently appropriate name, given our subsequent discovery of its homologies with the Quattro protein.

Fig. 1A shows the deduced protein sequences for Solo in three mammalian species. The GenBank accession numbers for the cDNAs and their associated proteins are AK074057 (human), AK131136 (mouse) and XM_341309 (rat). The RhoGEF and pleckstrin domain are at residues 1112–1274 and 1288–1394 in human Solo. The human, mouse and rat Solo proteins are highly conserved: between human and mouse identity is 89%, conservation is 92%; between mouse and rat identity is 94%, conservation is 97%. The homologies in the RhoGEF and pleckstrin domain are even higher. The RhoGEF domain is 91% identical between human and mouse, 95% identical between mouse and rat. The pleckstrin domain is 96% identical between human and mouse, 99% identical between mouse and rat. Fig. 1B shows the diverse C-termini resulting from alternative splicing of exons 22a and 22b. Fig. 1C depicts the homologies between human Solo and zebrafish Quattro. The fourth homology includes the RhoGEF and pleckstrin domains.

The human Solo cDNA corresponds to predicted human protein FLJ00128/FLJ10357 located on chromosome 14q11.2 on contig AL161668 (BAC R-998D10, library RPCI-11). Fig. 2 shows the genomic organization of human

Fig. 2. Genomic organization and splicing of the human and mouse Solo genes. Exon sizes are shown to scale in the top diagram. The start and stop codons are indicated. The lines above the exons depict major splicing events, those below depict minor splicing events (judged by both RT-PCRs and frequency of ESTs corresponding to each splicing decision). The miniexon between exons 22b and 23 unique to mouse is not shown. The accession numbers of the respective genomic sequences are AL161668 (BAC R-998D10, library RPCI-11) and AC079536.

Solo. Solo spans at least 23 kb of genomic sequence and consists of 25 translated exons. We do not yet know its promoter(s) or terminator(s). Table 1 shows the exon/intron organization of the Solo gene. Translated exon 3 differs in length between human and mouse/rat (1249 and 1237 nt, respectively) and its length is not a multiple of 3. The length of exon 3 is also unusual, since constitutive mammalian exons have a mean length of 137 nt, whereas alternative cassette exons with a restricted expression range deviate from this average (Zhang, 1998; Stamm et al., 2000). Therefore, exon 3 bears hallmarks of an alternatively spliced exon.

3.2. Solo transcript expression and alternative splicing

The Northern blots of Solo show two signals at approximately 6.5 and 7.5 kb. The former is ubiquitous but enriched in brain, whereas the latter is largely restricted to brain, though it is also very weakly visible in heart (Fig. 3A). The quantitations of the mouse developmental stage Northerns (Fig. 3B) show that both transcripts are observed in fetal and adult tissues. Their highest expression levels are in olfactory bulb and in cerebellum and they peak perinatally (from E16 to P0.5).

To establish which Solo exons are alternatively spliced, we performed RT-PCRs with human polyA$^+$ RNA from various tissues (Clontech) and primers covering the length of the gene. Human Solo exons 4–20 do not show alternative splicing. The tissues that we tested (fetal brain, adult whole brain, adult cerebellum and skeletal muscle) show two bands corresponding to 3$^+$ and 3$^-$ (Fig. 4A), a finding that we expected given its unusual length. The 3$^-$ band is particularly prominent in adult cerebellum (Fig. 4A, second lane from the right). Fetal brain shows multiple bands between the 3$^+$ and 3$^-$ species as well as a band below 3$^-$ marked as X (Fig. 4A, second lane from the left). Because the length of exon 3 is not a multiple of 3,

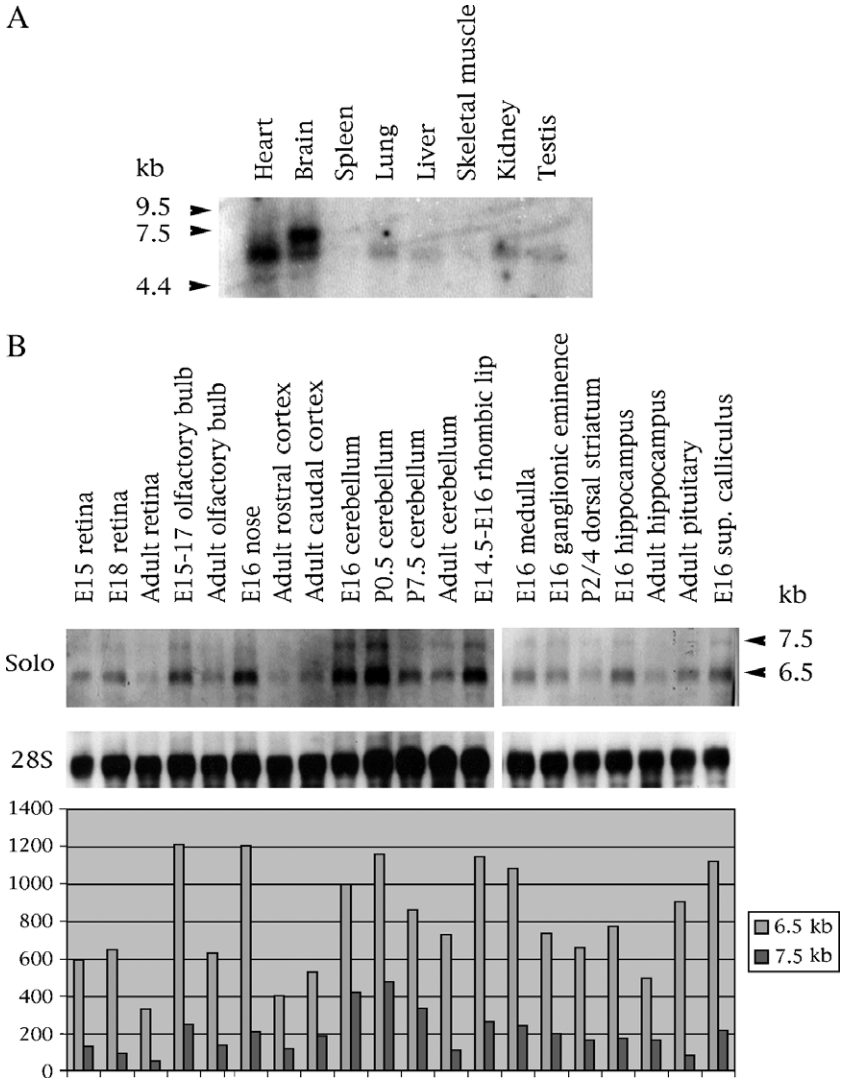

Fig. 3. Tissue and developmental expression of the Solo RNA. (A) Solo has two major transcripts: the 6.5 kb RNA is ubiquitous but enriched in brain, the 7.5 kb RNA is mostly restricted to brain. The multiple tissue Northern is rat (Clontech). (B) Solo mRNA in mouse brain compartments during development. Solo expression peaks perinatally (E16 and P0.5) in mouse. The numbers on the left of the graph represent signal intensity normalized against 28S rRNA.

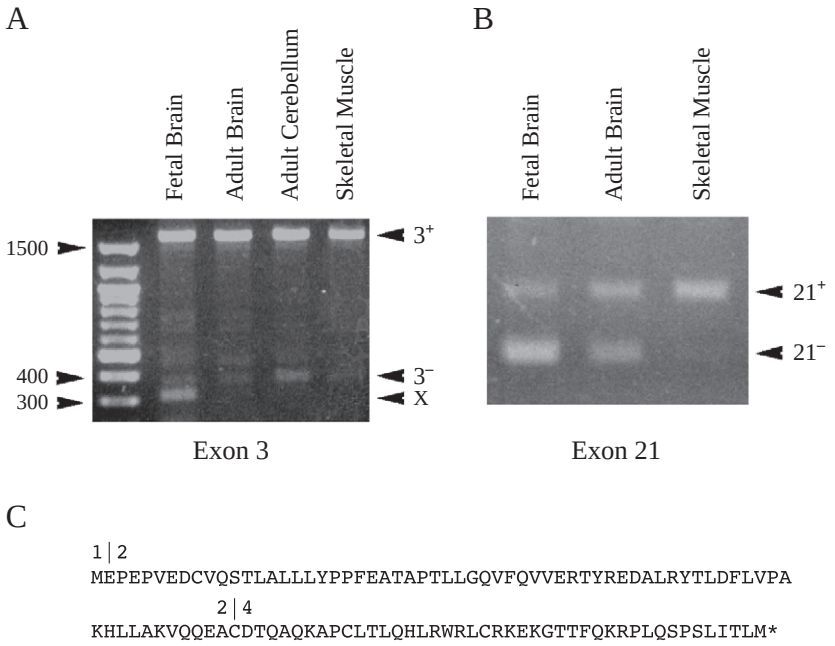

Fig. 4. Solo exons 3 and 21 are alternatively spliced. (A, B) RT-PCR of Solo in selected human tissues. (A) Primer pair: Solo-E2S/Solo-E4N. X indicates a species of unknown exact sequence. (B) Primer pair: Solo-E20S/Solo-E23N. (C) Exclusion of exon 3 creates a frameshift, resulting in premature termination of the Solo reading frame.

the reading frame shifts if it is excluded, resulting in premature termination of the Solo protein (Fig. 4C).

We also confirmed by RT-PCR that alternative splicing occurs in the 3′end of Solo, a fact we already knew from our cDNA clones and our surveys of the GenBank database (Fig. 4B). Exon 21 acts as a cassette, but its absence preserves the Solo open reading frame since its length is a multiple of 3. Interestingly, the band corresponding to 21^+ is prevalent in skeletal muscle, while the 21^- band is stronger in fetal brain.

Exons 22a and 22b appear to be mutually exclusive: we never found them together in the database, our clones or our RT-PCRs (data not shown). So far, we have documented the existence of human, mouse and rat Solo species corresponding to 21^+ $22b^+$ and 21^- $22b^+$ and of rat Solo species corresponding to 21^+ $22a^+$. In rodents, these splicing decisions give rise to two different C-termini due to the presence of stop codons in exons 22a and 23. In human Solo, exon 22a does not contain a stop codon, and so inclusion of either 22a or 22b produces C-termini ending within exon 23. However, because the length of 22b is an exact multiple of 3 whereas that of 22a is not, the termini (shown in Fig. 1B) differ in detail. The mouse Solo gene has an additional mini-exon of 21 nt between exons 22b and 23 which we found in several ESTs, but whose 3′splice site is not conserved in human.

3.3. Solo protein expression

For production of full-length Solo protein, exon 3 must be included, giving rise to a molecule of predicted molecular weight 165 kD and pI 5.46 prior to any modifications. Western blots of fetal brain show four bands corresponding to Solo: one is a closely spaced triplet at ~150 kD, whereas a singlet is visible at ~185 kD (Fig. 5, left lane). The various adult brain compartments (whole brain, cerebellum, cerebral cortex, hippocampus) show only the middle member of the triplet seen in fetal brain.

Solo gives a different profile in skeletal muscle. The signal is much stronger than that seen in fetal brain, which suggests skeletal muscle contains a significantly higher relative amount of Solo. This preferential expression is not seen in the Northerns (Fig. 3), implying that Solo may undergo selective post-transcriptional stabilization or enhanced translation in muscle. Solo protein in skeletal muscle migrates at 80, 115 and 150 kD.(Fig 5, top panel). The 150 kD band coincides with the top member of the

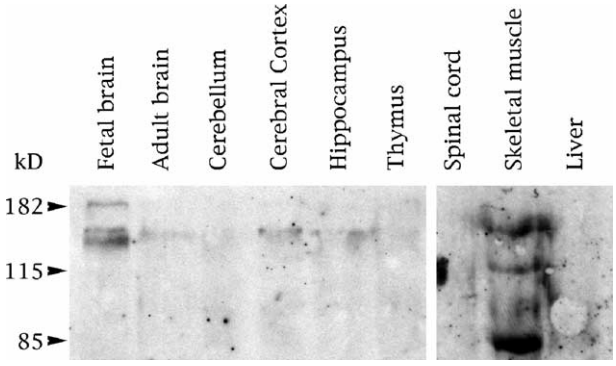

Fig. 5. Solo protein is expressed in the central nervous system and skeletal muscle and is more abundant in fetal than adult brain. The protein medleys are human (Clontech). Primary antibody: chicken IgY anti-Solo.

triplet seen in fetal brain. There is essentially no signal in thymus, spinal cord and liver. The Western patterns of Solo are the same whether we use anti-Solo antibodies raised in chicken (Fig. 5) or in rabbit (data not shown). The Western blot results suggest that Solo may undergo different regulatory and post-translation processes in different tissues.

We originally identified Solo in a two hybrid screen using a tau domain as bait. We were unable to confirm the interaction between Solo and tau by co-IPPs of either the exogenous or endogenous molecules in SY5Y cells. The endogenous result is not surprising, because Solo expression seems to be very low in most tissues and cell types. However, the lack of interaction of transfected (highly expressed) constructs suggests that the interaction between Solo and tau may be weak or transitory—or that tau is not a major interacting partner for Solo.

3.4. Intracellular localization of solo

The Western blot analysis shows that Solo is most highly expressed in fetal brain and skeletal muscle. We therefore decided to investigate Solo localization in two cell lines derived from tissues which show the highest relative expression of Solo: SY5Y (human neuroblastoma cells) and C2C12 (mouse myoblasts).

The pattern of Solo staining is similar in both cell types. The Solo signal is cytoplasmic and strongest around the nucleus (Fig. 6A and B, left panels), although in SY5Y the signal also extends into the processes. Use of the rabbit anti-Solo antibody showed the same pattern that we observed using chicken anti-Solo (results not shown). Pre-absorption with the respective peptide antigens shows that both antibodies are specific for Solo (data not shown).

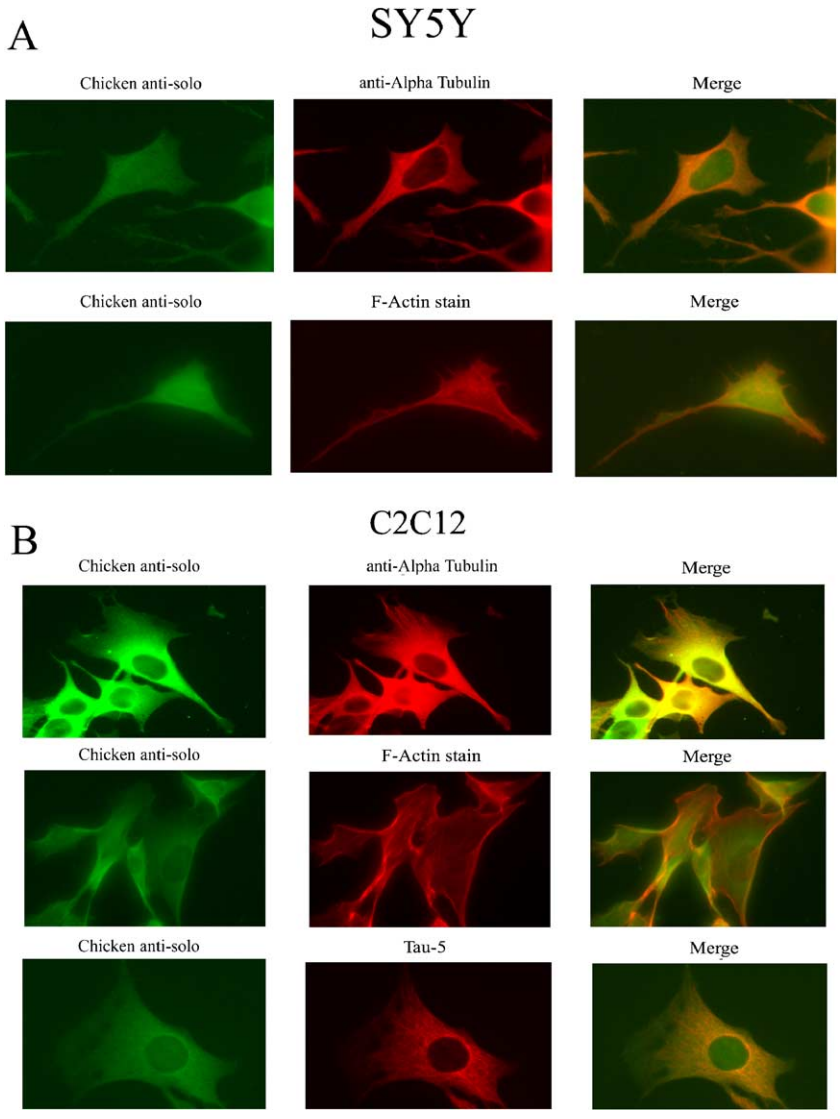

Fig. 6. The Solo protein shows a perinuclear localization in (A) SY-5Y human neuroblastoma and (B) C2C12 mouse myoblast cells. It partially co-localizes with cytoskeletal proteins tau, α-tubulin and f-actin but its staining pattern is punctate. The primary antibodies used are indicated above each panel.

To investigate if Solo is involved in cytoskeletal organization like several other RhoGEFs, we used immunocytochemistry to determine if it co-localizes with tau, α-tubulin and f-actin (Fig. 6A and B, center panels). The double staining did not show complete co-localization of Solo with any of these proteins (Fig. 6A and B, right panels). Also, the Solo staining is not fibrous, as is the case for tubulin and actin, but punctate. The Solo signal is congruent with preferential localization in the perinuclear region, which suggests possible involvement in functions of the endoplasmic reticulum.

4. Discussion

Rearrangements of the cytoskeleton, which consists of actin filaments, microtubules, and intermediate filaments, are required for various cellular processes, such as morphology changes, migration, adhesion and cytokinesis (Etienne-Manneville, 2004). These temporal and spatial reorganizations of cell structure and cell contacts can be stimulated by extracellular signals, including growth factors, hormones, and other biologically active substances. Members of the Rho GTPase family of low-molecular-weight GTP binding proteins, which include Rho, Rac and Cdc42 are known to regulate cell shape, growth, adhesion and motility (Govek et al., 2005; Raftopoulou and Hall, 2004; Wennerberg and Der, 2004). These small GTPases are activated by large guanine nucleotide exchange factors (GEFs) that promote the exchange of GDP for GTP, while the activation state is negatively regulated by GTPase activating proteins.

Many GEFs for Rho GTPases (abbreviated as RhoGEFs) have been identified, forming a family with ~60 members (Schmidt and Hall, 2002). Several of these GEFs, including the prototype Dbl, were first identified as oncogenes (Cerione and Zheng, 1996). A common feature of RhoGEFs is a GEF domain responsible for exchange activity, followed by a pleckstrin homology (PH) domain thought to be involved in GEF localization (Hoffman and Cerione, 2002). Most of the family members are expressed preferentially in specific tissues and developmental stages, suggesting involvement in specific events (Cerione and Zheng, 1996; Whitehead et al., 1997). Several RhoGEFs (such as Trio/unc73/kalirin) also act as serine/threonine kinases which regulate migration and axon guidance in neurons (Bateman and Van Vactor, 2001).

Our analysis of Solo reveals that it also has a GEF and an adjacent downstream PH domain in its C-terminal region, which makes it a member of the RhoGEF family. Intriguingly, there is no further homology between Solo and other mammalian RhoGEFs whereas it shares additional regions of homology with yet another newly discovered molecule, Quattro, which is thought to modulate actin filament dynamics during zebrafish embryo morphogenesis (Daggett et al., 2004).

Because the N-terminus of Quattro is novel, Daggett et al. suggested that Quattro may be a founding member of a new family of previously unidentified RhoGEFs, which are most closely related to the kalirins (which include Trio) and the Dbl family (which contains Duo). Solo's homology with Quattro (Fig. 1C) indicates that these two molecules may belong to the same RhoGEF family. It also implies Solo may be the human equivalent of Quattro and may have a function in mediating interactions between the cytoskeleton and signal transduction molecules of the Rho/Rac family.

Solo contains an unusually large exon (#3) whose length is not a multiple of three and which behaves as a cassette. If exon 3 is excluded, the resulting frameshift is in-frame with a premature stop codon which would produce a truncated Solo protein lacking the GEF and PH domains. Our RT-PCR analysis suggests that this alternative splicing event occurs in some tissues. The corollary is that Solo may be using alternative splicing as a way to regulate the activity of its protein, perhaps through nonsense-mediated decay of its RNA—a mechanism used by several other alternatively spliced genes (Lewis et al., 2003; Maquat, 2004).

The results from Northern and Western analyses indicate that Solo is preferentially expressed in brain and that its levels are highest in perinatal cerebellum, making its developmental profile similar to that of Trio (Ma et al., 2005). Many RhoGEFs are expressed in the nervous system during development with distinct spatial and temporal patterns (Yoshizawa et al., 2003). This expression profile suggests that Solo may play a role in the development of the nervous system, as is the case with many RhoGEF proteins including Quattro (Bateman and Van Vactor, 2001; Daggett et al., 2004).

Besides its presence in various brain components, Solo protein is also highly expressed in human adult skeletal muscle, although Solo mRNA does not seem to be strongly expressed in the same tissue. This, together with the fact that the Solo protein found in adult skeletal muscle differs from that observed in fetal brain, suggests that Solo may undergo selective post-transcriptional processing and stabilization in muscle. Trio has also been implicated in the control of skeletal muscle development (Schmidt and Hall, 2002).

Our ICC studies show that endogenous Solo is found in the perinuclear region of cells, although in neuroblastoma SY5Y cells it also extends into the processes. Interestingly, proto-Dbl also displays a perinuclear pattern whereas activated onco-Dbl, which lacks the N-terminal domain, co-localizes with actin (Bi et al., 2001), suggesting the N-terminal of Dbl plays a role in determining the localization as well as the activities of Dbl. Similarly, full-length Solo does not completely co-localize with the three cytoskeletal elements that we tested (tau, actin and tubulin). It is possible that endogenous Solo may exert an autoinhibitory effect on its localization and activity through its N-terminus.

This study provides the basic framework for understanding the roles of this novel RhoGEF in cytoskeletal interactions and neuronal development. In future studies we

will enlarge our understanding of Solo's function, activity and substrates.

Acknowledgments

This study was supported by NICHD grant HD05515 to A.A. and P.M. We wish to thank John Memmott for expert technical assistance.

References

Bateman, J., Van Vactor, D., 2001. The Trio family of guanine-nucleotide-exchange factors: regulators of axon guidance. J. Cell. Sci. 114, 1973–1980.

Bi, F., Debreceni, B., Zhu, K., Salani, B., Eva, A., Zheng, Y., 2001. Autoinhibition mechanism of proto-Dbl. Mol. Cell. Biol. 21, 1463–1474.

Cerione, R.A., Zheng, Y., 1996. The Dbl family of oncogenes. Curr. Opin. Cell Biol. 8, 216–222.

Daggett, D.F., et al., 2004. Developmentally restricted actin-regulatory molecules control morphogenetic cell movements in the zebrafish gastrula. Curr. Biol. 14, 1632–1638.

Erickson, J.W., Cerione, R.A., 2004. Structural elements, mechanism, and evolutionary convergence of Rho protein-guanine nucleotide exchange factor complexes. Biochemistry 43, 837–8342.

Etienne-Manneville, S., 2004. Actin and microtubules in cell motility: which one is in control? Traffic 5, 470–477.

Govek, E.E., Newey, S.E., Van Aelst, L., 2005. The role of the Rho GTPases in neuronal development. Genes Dev. 19, 1–49.

Hoffman, G.R., Cerione, R.A., 2002. Signaling to the Rho GTPases: networking with the DH domain. FEBS Lett. 513, 85–91.

Le Douarin, B., Nielsen, A.L., You, J., Chambon, P., Losson, R., 1997. TIF1 alpha: a chromatin-specific mediator for the ligand-dependent activation function AF-2 of nuclear receptors? Biochem. Soc. Trans. 25, 605–612.

Lewis, B.P., Green, R.E., Brenner, S.E., 2003. Evidence for the widespread coupling of alternative splicing and nonsense-mediated mRNA decay in humans. Proc. Natl. Acad. Sci. U. S. A. 100, 189–192.

Luo, M.H., Tse, S.W., Memmott, J., Andreadis, A., 2004. Novel isoforms of tau that lack the microtubule-binding domain. J. Neurochem. 90, 340–351.

Ma, X.M., Huang, J.P., Eipper, B.A., Mains, R.E., 2005. Expression of trio, a member of the Dbl family of Rho GEFs in the developing rat brain. J. Comp. Neurol. 482, 333–348.

Maquat, L.E., 2004. Nonsense-mediated mRNA decay: splicing, translation and mRNP dynamics. Nat. Rev., Mol. Cell Biol. 5, 89–99.

Raftopoulou, M., Hall, A., 2004. Cell migration: rho GTPases lead the way. Dev. Biol. 265, 23–32.

Schmidt, A., Hall, A., 2002. Guanine nucleotide exchange factors for Rho GTPases: turning on the switch. Genes Dev. 16, 1587–1609.

Stamm, S., Zhu, J., Nakai, K., Stoilov, P., Stoss, O., Zhang, M.Q., 2000. An alternative-exon database and its statistical analysis. DNA Cell Biol. 19, 739–756.

Wennerberg, K., Der, C.J., 2004. Rho-family GTPases: it's not only Rac and Rho (and I like it). J. Cell. Sci. 117, 1301–1312.

Whitehead, I.P., Campbell, S., Rossman, K.L., Der, C.J., 1997. Dbl family proteins. Biochim. Biophys. Acta 1332, F1–F23.

Yoshizawa, M., et al., 2003. Dynamic and coordinated expression profile of dbl-family guanine nucleotide exchange factors in the developing mouse brain. Gene Expr. Patterns 3, 375–381.

Zhang, M.Q., 1998. Statistical features of human exons and their flanking regions. Hum. Mol. Genet. 7, 919–932.